

# Catalog of dynamic electromagnetic spectra

Christian Monstein<sup>1, 2, 3</sup>

<sup>1</sup> Istituto ricerche solari Aldo e Cele Daccò (IRSOL), Università della Svizzera italiana, Locarno, Switzerland

<sup>2</sup> Institute for Particle Physics and Astronophysics, ETH Zurich, Switzerland

<sup>3</sup> Monstein Radio Astronomy Support, Freienbach, Switzerland

e-mail: cmonstein(at)swissonline.ch

Draft 30.04.2011 / Updated 04.10.2015, 10.10.2016 , 14.05.2019, 27.01.2020, 14.06.2020, 16.05.2022, 14.11.2023, 18.03.2024

**Abstract.** This catalog demonstrates dynamic electromagnetic spectra observed by Callisto, Phoenix-3 and ARGOS radio spectrometers. In the first part natural spectra are presented while in the second part we concentrate on artificial (man-made) spectra. This catalog shall help the scientist to detect and identify weak solar radio bursts in highly interfered spectra as well as to separate natural dynamic time-frequency structures from man made rfi. In addition, Callisto spectrometers have proven to be a cheap and reliable instrument for radio frequency monitoring of terrestrial interference.

**Key words.** Callisto, radio spectrum, interference, solar bursts.

## 1. Introduction

A catalog of different electromagnetic spectra is firstly presented for the convenient interpretation of dynamic radio observations of solar flares in view of International Space Weather Initiative (ISWI). Secondly, this catalog shall also help to distinguish fast radio bursts (FRB) of extra solar origin from man made interference. Spectra are observed at different locations worldwide and with different antenna systems within the e-Callisto network (Benz , 2004). Observations took place since 2004. The catalog consists of spectrograms all produced in the same way: bad channels with high  $\sigma$  eliminated, background subtracted, and zoomed to the visually interesting part.

## 2. Solar spectra

In the collection below most of the typical solar radio bursts will be presented and shortly discussed. A detailed description of the physics behind the bursts can be found in the publication by Kundu (Kundu , 1965).

### 2.1. Type I bursts (noise storm)

A noise storm consists of long series of short and narrow-band bursts continuing over hours or days. Polarization is always high (circular) and the sign of the polarization can change within one day. The bursts are superimposed on a background of slowly varying enhanced radiation which

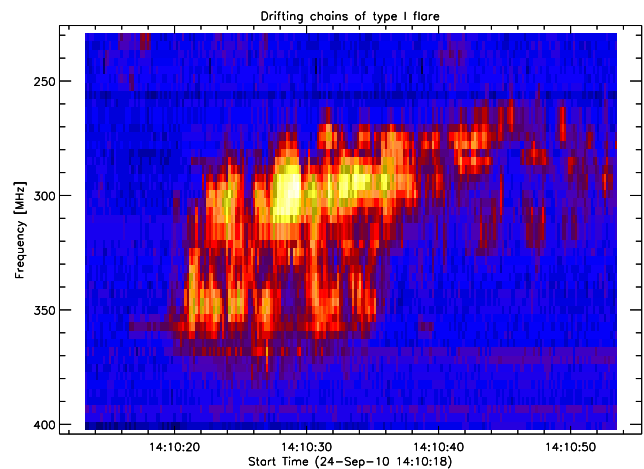


**Fig. 1.** Noise storm of solar radio emission observed at Bleien observatory, Switzerland. Antenna = dish 7 m, circularly polarized. A chain of type I bursts is shown.

has been described as a "continuum", although it is possible that the background may itself be composed of a large number of overlapping bursts (?). Noise storms are normally spread over a large frequency band but are rarely seen above 350 MHz. On many occasions the bursts have bandwidths of a few MHz and lifetimes extending from 0.1 seconds to 1 second. Chains of bursts last nearly 1 minute (Fig. 1). At frequencies below 40 MHz drifting bursts of bandwidth up to 30 MHz and lifetimes less than a second may predominate.

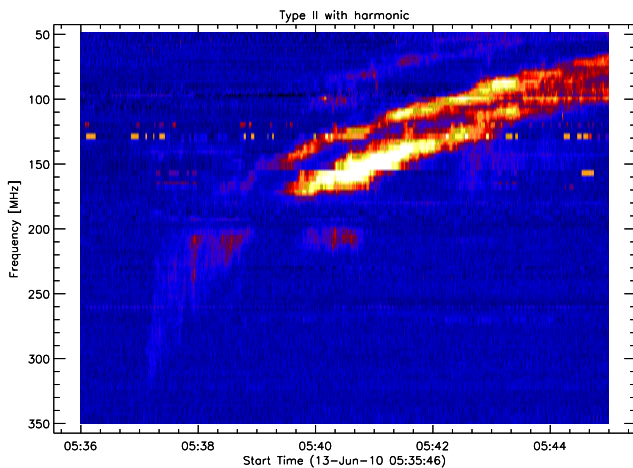


**Fig. 2.** Type II solar radio flare with harmonics observed at Ooty observatory, India. Antenna = logarithmic-periodic linear polarized.

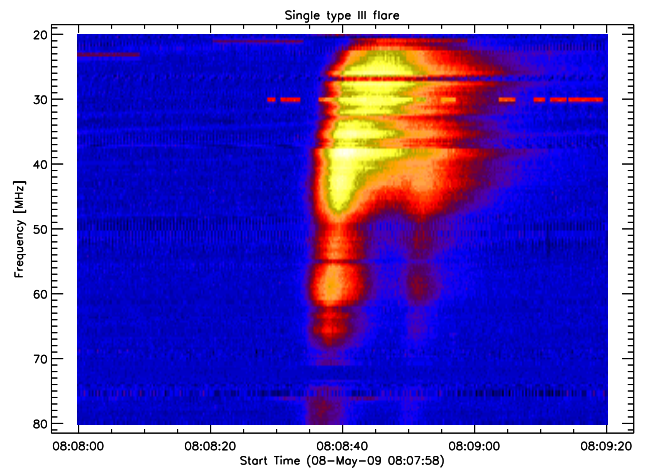


**Fig. 4.** Two low-frequency isolated type III solar radio bursts observed at Bleien observatory, Switzerland. Antenna = logarithmic-periodic CLP-5130.

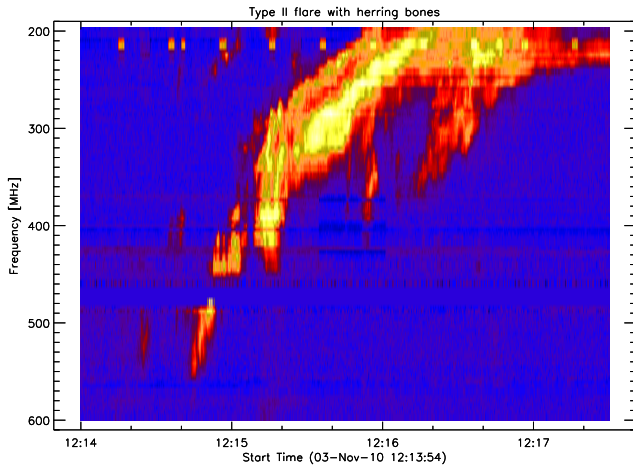


**Fig. 3.** Type II solar radio flare with harmonics and 'herring bones', observed at Bleien observatory, Switzerland. Antenna = parabolic dish 7 m, circular polarized.

## 2.2. Type II bursts (slow drift)

After large flares narrow bands of intense radiation drift sometimes slowly, and often irregularly, towards lower frequencies. Figure 2 shows a typical example. The spectra occasionally show the presence of a second harmonic in frequency, but are often so complex as to preclude such identifications. In rare cases type II bursts show a characteristic called 'herring bones' as illustrated in Figure 3. (xxxEs gibt ein viel schöneres Beispiel von Birr am 22. September 2011xxx). The velocity of the solar disturbance giving rise to these slow-drift bursts may be deduced from their rate of change of frequency. This velocity is of the order of 1000 km/s and corresponds to supersonic shocks originating in the flare or coronal mass ejection (CME) and moving through the corona.

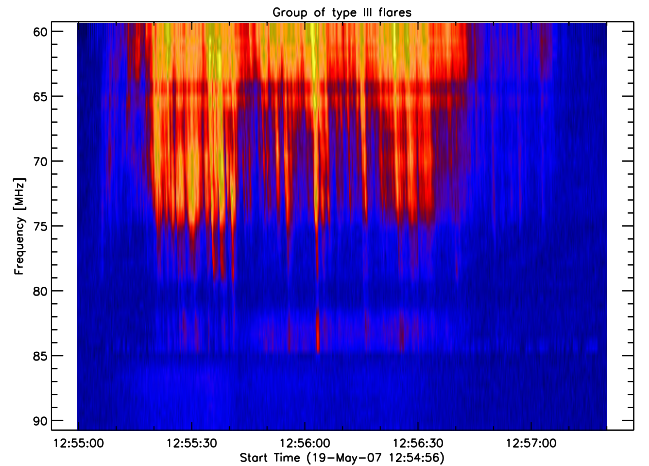


**Fig. 5.** Group of type III solar radio bursts observed at Bleien observatory, Switzerland. Antenna = log-per CLP-5130, linearly polarized. Some type III are reverse drifting.

## 2.3. Type III bursts (fast drift)

Fast drifting bursts, a very commonly occurring phenomenon, have typical durations of a second. The duration increases at lower frequency and the drift rate (MHz/s) decreases. Type III bursts typically occur in groups of 3 to 10 with a total duration of less than 60 sec, as illustrated in Figures 4-6. The radio emission is caused by flare accelerated electron beams propagating through the corona at high velocity (up to half the speed of light).

## 2.4. Type IV bursts

The continuum radiation is a steady enhancement of the background level over a wide band of the spectrum, and is often followed by a noise storm (type I). At times, however, an extremely intense form of continuum radiation is observed covering a frequency band of more than 300 MHz, see figure 7. It often occurs during and after great out-

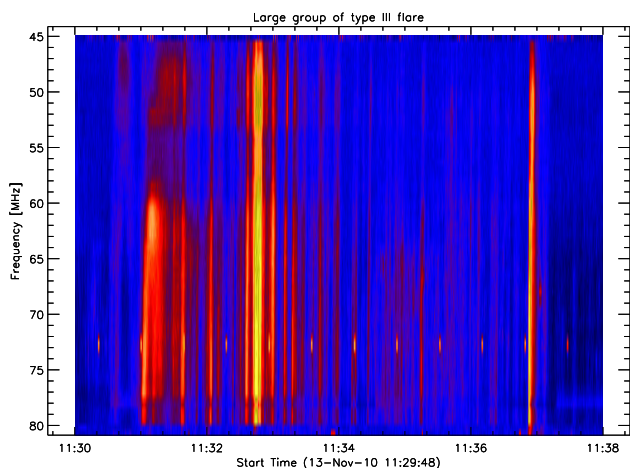


**Fig. 6.** Large group of type III solar radio flare observed at Humain observatory, Belgium. Antenna = log-per CLP-5130, linearly polarized. Probably a U-burst on the left side near 11:31UT.

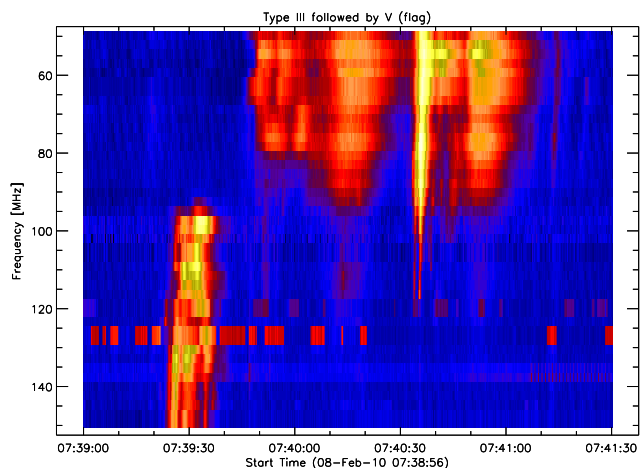


**Fig. 8.** Type V solar radio burst observed at Ooty observatory, India. Antenna = home made, linearly polarized, pointing to zenith.

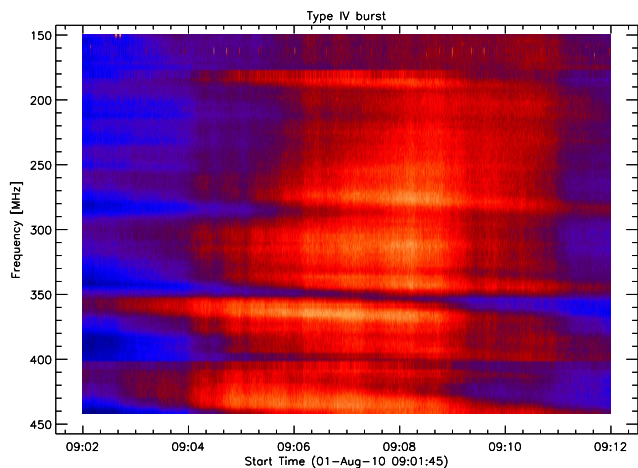


**Fig. 7.** Type IV solar radio flare (continuum) observed in Badary observatory near Irkutsk, Russian Federation. Antenna = log-per CLP-5130, linearly polarized.

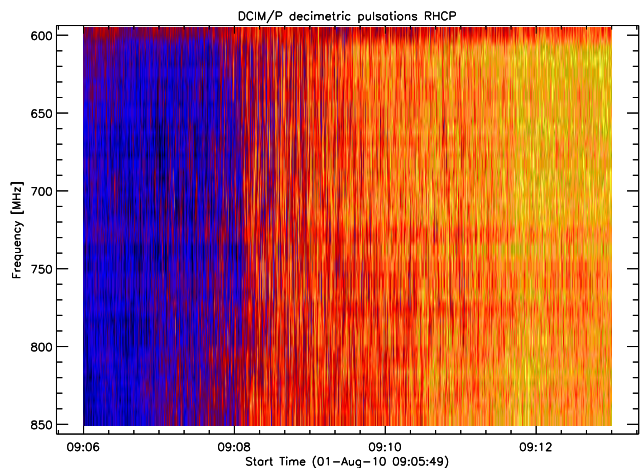


**Fig. 9.** DCIM (decimetric) solar radio burst with pulsations observed at Bleien observatory, Switzerland. Antenna = 7 m dish, circularly polarized RHCP, pointing to sun.

bursts, and may last 10-300 minutes. The wavy, periodic intensity variations in frequency are **not** caused by standing waves in the receiving system. They are not properties of the type IV burst. This can be confirmed by comparing the same flare from observations at different locations (e-Callisto network).

## 2.5. Type V bursts

Type V bursts are always associated with type III bursts and follow them for a few tens of seconds. They appear like a flag attached at low frequency to the type III burst, see Figure 8 near 07:39:30UT. The emission is quasi continuous with a bandwidth of less than the type III burst. Duration is typically less than 1 minute. The exciter is the electron beam that is partially scattered at high altitude.

## 2.6. Type DCIM/P bursts

Decimetric bursts are quite frequent and cover frequency ranges of up to a one GHz. In figure 9 we can see pulsations in right circular polarization while at the same time left circular polarization is not pulsed but shows continuum, see figure 10. The origin of the emission needs to be investigated further.

## 2.7. Type DCIM/F burst

Intermediate drift burst of a DCIM event produced by a X6.9 flare covering hundreds of MHz frequency up to 4 GHz. In figure 11 we can see fiber-like structures. Therefore also the name fiber burst. This flare was recorded with Phoenix-3, a wide band high speed FFT-spectrometer.

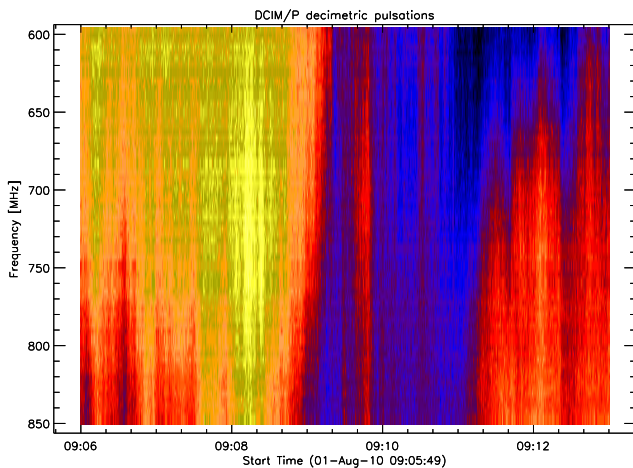


**Fig. 10.** Decimetric (DCIM) solar radio burst with continuum observed at Bleien observatory, Switzerland. Antenna = 7 m dish, circularly polarized LHCP, pointing to sun.

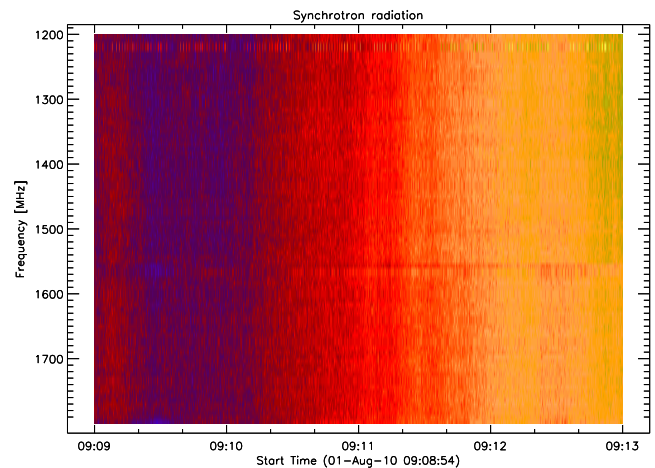


**Fig. 12.** Gyro-synchrotron solar radio radiation observed in L-band at Bleien observatory, Switzerland. Antenna = 5 m dish, linearly polarized, pointing to sun.

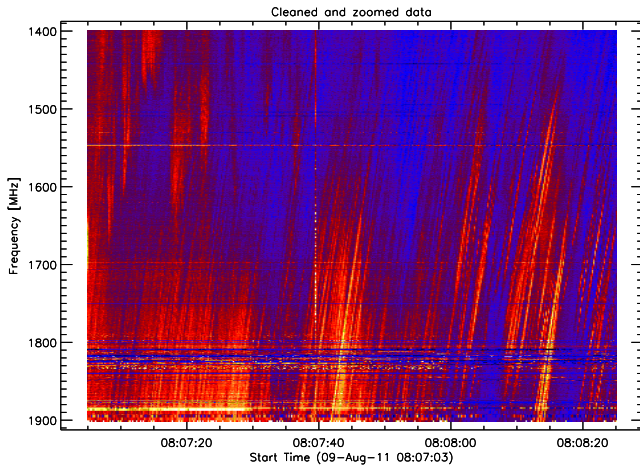


**Fig. 11.** DCIM (decimetric microwave) solar radio flare with fiber structures observed at Bleien observatory, Switzerland. Antenna = 5 m dish, pointing to sun.

## 2.8. Synchrotron radiation

Decimetric continuum or synchrotron radiation during active sun produce intensive broad band noise, see figure 12. Contrary to other sources in astrophysics, the majority of solar flare electrons reach only mildly relativistic energies. Thus the emission is called gyro-synchrotron. These electrons easily radiate due to gyration without any collisions with other particles. They radiate via the cyclotron (non-relativistic), synchrotron, and possibly inverse-Compton radiation mechanisms. The gyro-synchrotron radiation mechanism depends on the strength of the magnetic fields. These fields are present everywhere, but they tend to be stronger in those places where electrons are accelerated to high energies, thus helping the high efficiency with which these electrons emit radiation

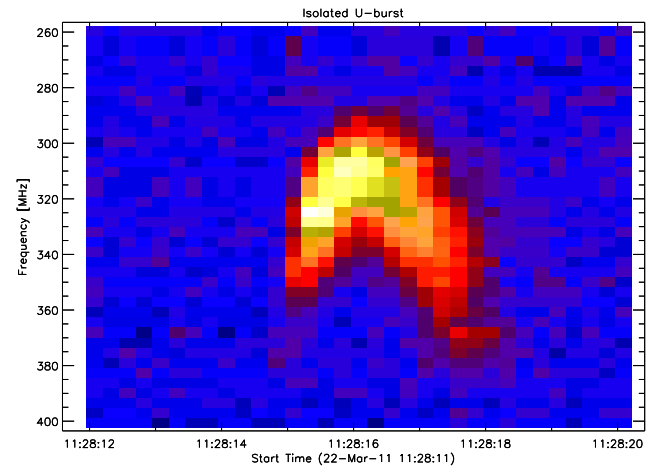


**Fig. 13.** U-burst in intensity (LHCP+RHCP). Antenna = 7 m dish at Bleien observatory, circular polarized, pointing to the Sun.

## 2.9. Type U burst

The U-burst, first identified by Maxwell and Swarup and Haddock (Maxwell, 1958), is a type of solar event lasting up to about 10 sec in which the frequency or the emission first drifts rapidly downwards, then increases again. On the dynamic spectrum the burst has appearance of an inverted letter U, see figure 13. The frequency drift rate at the sides of the 'U' is of the same order as that observed in ordinary type III bursts; the U-burst is now generally regarded as sub-class of type III, and is believed to be generated by plasma waves set up by fast electron streams in the solar corona following a loop-shaped magnetic field that turns back to the chromosphere.

## 2.10. Interference from ground reflection

Interference from ground happens only in linear horizontal polarization if the ground is reflective due to water,

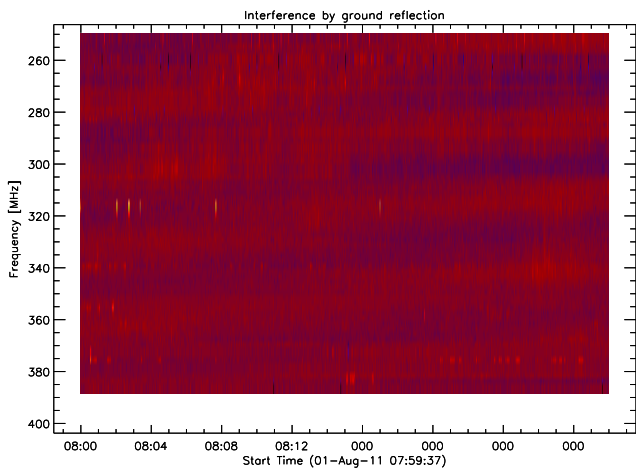


**Fig. 14.** Interference due to reflection of the solar radiation on the ground. Antenna = log-per at station Humain of Royal Observatory of Belgium (ROB), linearly polarized, pointing to sunrise.

metal or plants. Also buildings or other large constructions may lead to interference effects. This happens mainly during sun-rise and sun-set when the elevation of the sun is low, thus when the reflected radiation and the direct radiation are both in the beam of the antenna, see figure 14. Detectable interference from solar radiation proves that the quiet solar flux can be measured. Thus, the system is sensitive down to quiet solar flux.

### 2.11. Interference from reflection on water

Interference from water happens only in linear horizontal polarization. This happens mainly during sun-rise and sun-set when the elevation of the sun is low, thus when the reflected radiation and the direct radiation are both in the beam of the antenna, see figure 15. Detectable interference from solar radiation proves that the quiet solar flux can be measured. Thus, the system is sensitive down to quiet solar flux.

### 2.12. Terrestrial lightning

During local thunderstorms the telescope receives electromagnetic radiation from lightning strokes. They have similar structure as solar type III bursts, see figure 16. Assuming that these waves were generated by some kind of Dirac-pulse, the spectrum must be broad band and flat, thus lightning strikes could be used to calibrate standing waves of the telescope.

### 2.13. Ionospheric caustics

Very rare distorted solar type I bursts due to focusing of the burst in the ionosphere, see figure 17. On December 12th 2013 NOAA reported between 08:04 and 12:08 only radio noise at 245 MHz observed in San Vito. But some European observatories of the e-Callisto net-

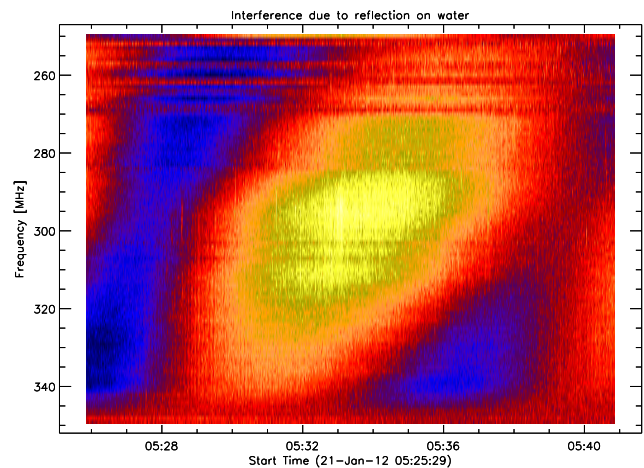


**Fig. 15.** Interference due to reflection of the solar radiation on the surface of a sea. Antenna = group of 4x4 Yagis at Crimea island Ukraine, linearly polarized, pointing to sunrise.

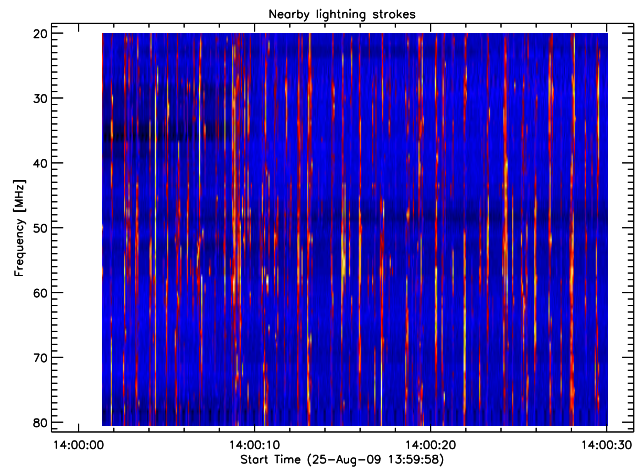


**Fig. 16.** Broad band radiation generated by nearby lightning strokes observed at Bleien observatory, Switzerland. Antenna = biconical dipole, linearly polarized.

work (Germany, UK and Ireland) observed very strange reverse drifting and V-type bursts which was never recognized by the author before. Private communication showed that these strange structures are due to focusing effects in the ionosphere. *Abstract from C. Mercier, F. Genova and M. G. Aubier Annales Geophysicae, 1989, 7, (2), 195-202: The effects of traveling ionospheric disturbances (TID's) on the observations of solar radio storms at decameter wavelengths by the radioheliograph array in Nançay are used to derive basic parameter of atmospheric gravity waves. TID's are modeled as one-dimensional lenses, which produce apparent shifts of the source positions at meter wavelengths, and focusing at decameter wavelengths.* Interestingly it is possible to observe complex ionospheric behavior with cheap and simple radio-telescopes like Callisto. People who are interested in such kind of observations to study ionospheric gravity waves should generate observing programs for frequencies below

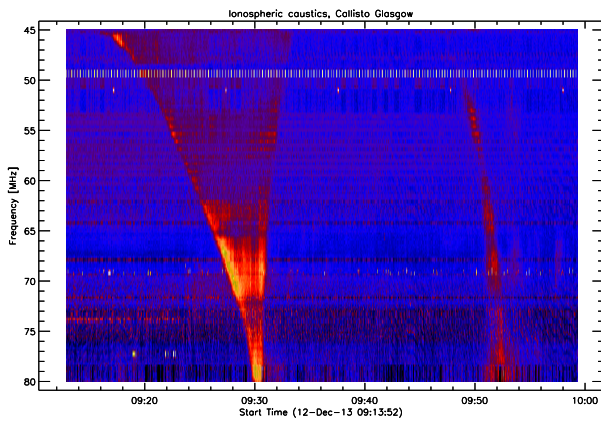


**Fig. 17.** Ionospheric caustics observed in Glasgow/UK with Callisto and a LPDA.

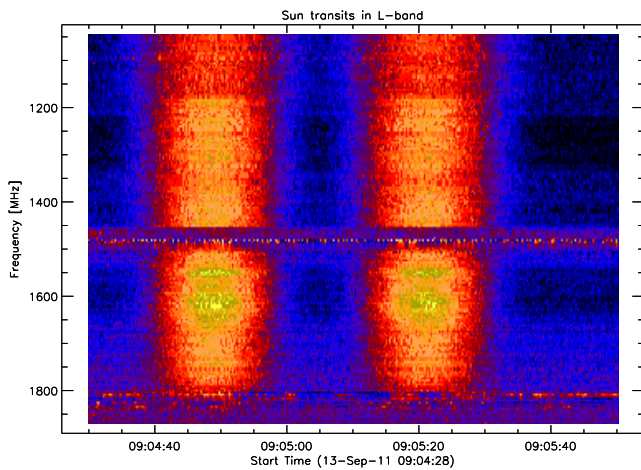


**Fig. 18.** Sun transits observed with Callisto at Bleien observatory, Switzerland. Antenna = 5 m dish circular polarized (LHCP).

100 MHz, ideally with an additional up-converter for frequencies from 15 MHz - 100 MHz.

#### 2.14. Microwave pulsations

tbđ

#### 2.15. Transit quiet sun

Sun transit observed during a test procedure on a new series of Callisto spectrometer connected to a L-band heterodyne-converter. The transits are artificially performed by a special function called 'passage' within the antenna control software. Low sensitivity near 1500 MHz due to fast switching of internal receivers, see figure 18. Strong interference (horizontal lines) above 1800 MHz due to a nearby mobile phone relay station.

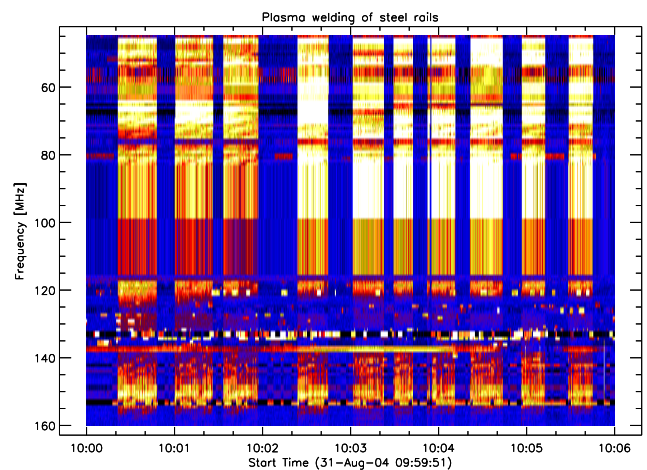


**Fig. 19.** Interference due to manual plasma welding near the telescope observed at Bleien observatory, Switzerland. Antenna = log-per CLP-5130, linearly polarized  $45^\circ$ .

### 3. Artificial (man-made) spectra

#### 3.1. Electric (Plasma) welding

To the end of August 2004 new rails were installed to secure our scaffold at both telescopes in Bleien. The rails had to be welded together with an electric plasma welding tool. While the welding operator was working, all instruments were operational and we got very strong interference due to the electromagnetic fields of the fast changing current in the connecting wiring. Assuming that these interference is broad band one could try to use this pseudo-flare for calibration.

#### 3.2. Electric fence

The nearby farmer uses an electric fence to keep his cows within a meadow near the telescopes during summer for feeding. The electric fence had a distance of about 5 m to the telescopes. Sparks between wire and large blades of grass lead to short and intensive electromagnetic fields producing bright pixels in the spectra, see figure 20. These bright pixels are pseudo-periodic and appear as diagonal structures in the spectrum from bottom left to top right. After discussions with the farmer, the electric fence was switched off when no cows were around.

#### 3.3. Damaged GAL (gate array logic)

A very time consuming problem occurred in November 2008. Some periodic structure like a U-burst in L-band with a time period of about 15 seconds, see figure 21. Only with some highly sophisticated measuring equipment of OFCOM it was possible to identify the source. It was a damaged GAL (gate array logic) in the front-end control board of the 5 m dish at Bleien observatory. After replacement of the pre-programmed GAL everything was o.k. again.

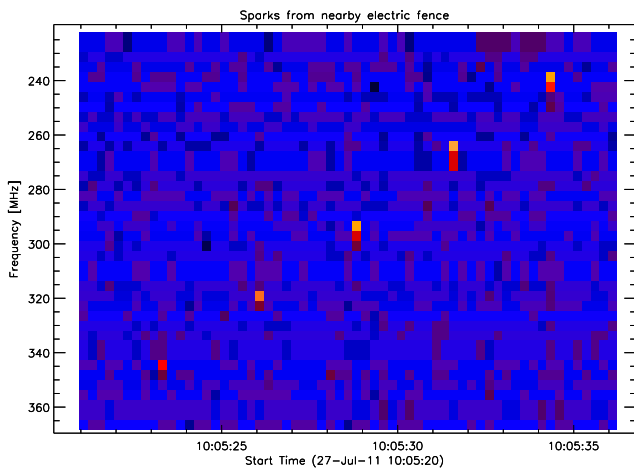


**Fig. 20.** Interference due to electric fence near the telescope observed at Bleien observatory, Switzerland. Antenna = parabolic dish 7 m, linearly polarized  $45^\circ$ .

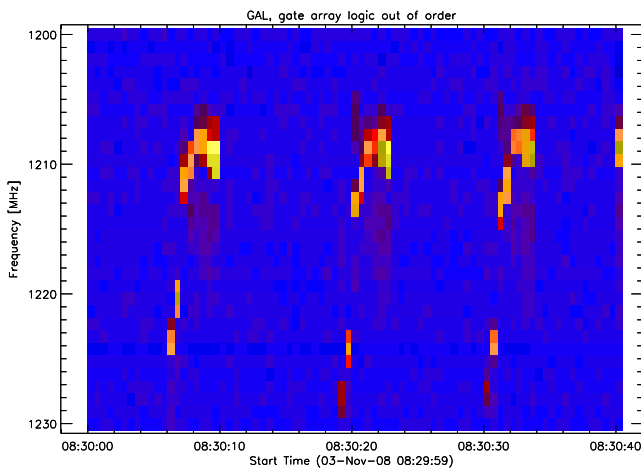


**Fig. 21.** Interference due to damaged gate array logic in the front-end of the telescope observed at Bleien observatory, Switzerland. Antenna = parabolic dish 5 m, linearly polarized  $45^\circ$ .

### 3.4. Broken component in radiometer)

Strong, periodic interference (small vertically oriented lines) due to faulty component in a radiometer at Metsähovi Radio Observatory (MRO) in Finland, see figure 22.

### 3.5. Damaged Mini Circuits pre-amplifier

Another very time consuming problem occurred in mid 2011. Some strange, very strong low frequency interference with a time period of about 10 milliseconds appeared on all observed frequencies, see figure 23. After many month of investigation, technicians from MRT found the source of rfi. It was a damaged pre-amplifier from MiniCircuits company which started to oscillate after a lightning stroke hit the antenna. After replacement of the pre-amplifier everything was o.k. again.

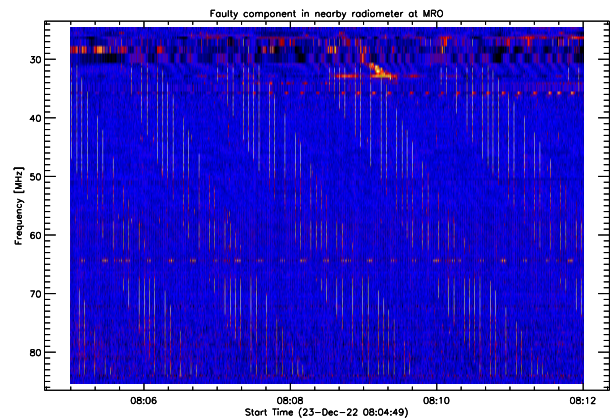


**Fig. 22.** Strong, periodic interference due to faulty component in a radiometer at Metsähovi Radio Observatory (MRO) in Finland.

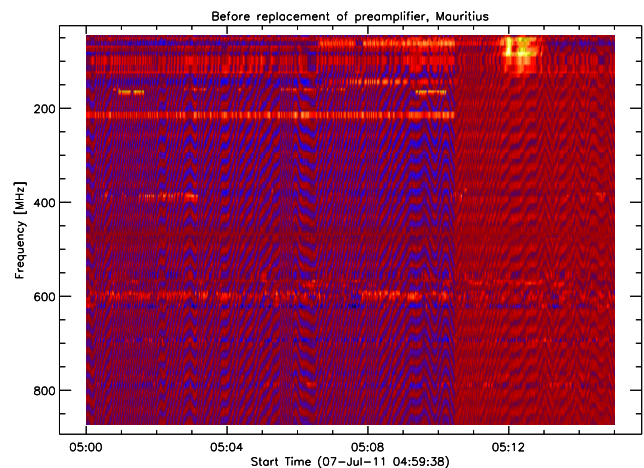


**Fig. 23.** Interference due to damaged pre-amplifier in the front-end of the telescope observed at MRT observatory, Mauritius. Antenna = large log-per, linearly polarized pointing to sky. Type III solar flare top right with about 30 sfu (300'000 Jansky).

### 3.6. Interfering LED driver

After installation of a new Callisto spectrometer at Metsähovi observatory we got an extremely high level of interference below 1 GHz, see figure 24. It took more than one month to find out the source of the radiation. It was a simple driver circuit for LED illumination in the observatory. After replacing this non-conform circuit, the spectrum was clean and free from interference as one would expect in a radio protected zone.

### 3.7. Doppler shifted transponder of SMART-1

In September 2nd 2006, the ESA satellite SMART-1 was observed during its perilunar orbit before crashing onto the moons surface. The plot shows the doppler shifted down-link signal of the S-band transponder, see figure 25. The observed frequency range at the rf-level was between 2230 MHz and 2239 MHz. The plot shows the down-

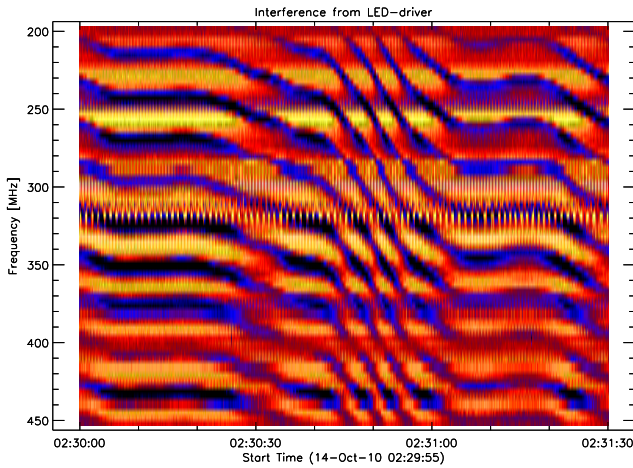


**Fig. 24.** Interference due to LED-driver circuit near the telescope observed at Metsähovi observatory, Finland. Antenna = log-per DVB-T like, linearly polarized.

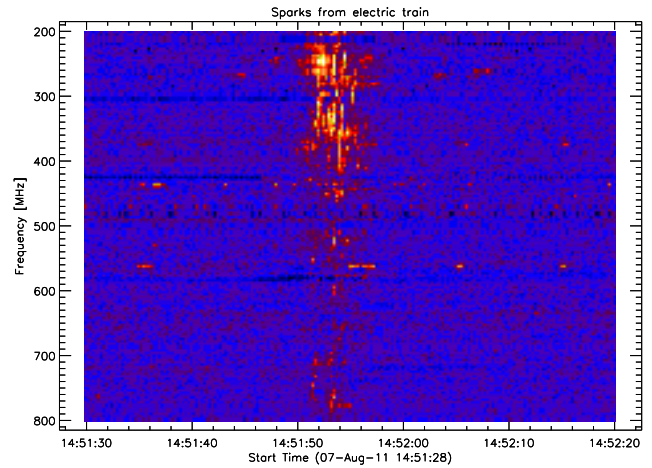


**Fig. 26.** Quasi burst caused by a nearby electric train of Südostbahn(SOB). Antenna = log-per, linearly polarized.

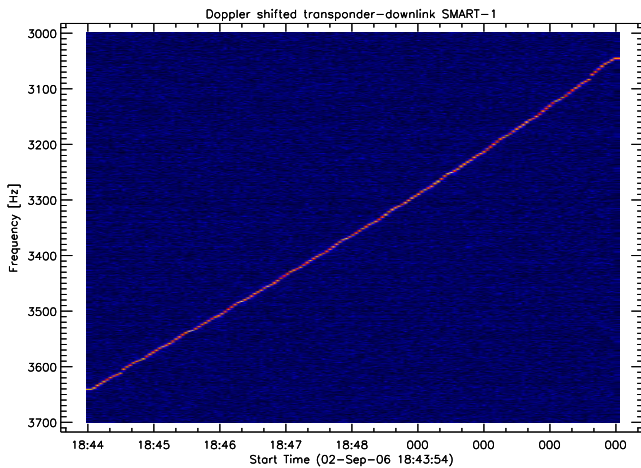


**Fig. 25.** Weak transponder signal from SMART-1 in its per-lunar orbit. Antenna = 5 m dish, linearly polarized.

converted (AR5000) frequency shifted into the audio-range (KHz) of a sound-card FFT-spectrometer.

### 3.8. Electric arc on pantograph of an electric train

This event is not a burst at all, it just looks like a solar noise storm or type I burst. In fact it's completely man-made caused by bad electric contact between pantograph of the train and the power line and/or bad contact of the wheels to the rails. This burst doesn't show any periodic structure.

### 3.9. 'Necklace' burst

The 'necklace'-burst is of non solar origin at all, it just looks like a regular pulsating solar burst. In fact it's completely man-made by quasi-periodic interruptions of an electric current or ignition sparks. Possible sources are chain saw, electric drill, motor cycle etc.

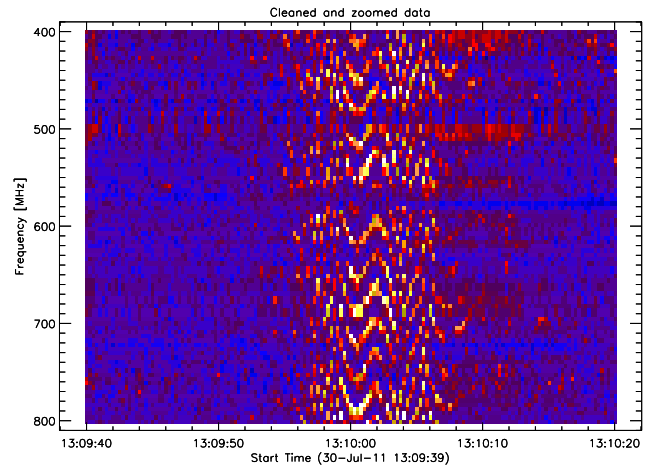


**Fig. 27.** Necklace burst man made by a motor cycle. Antenna = log-per, linearly polarized.

### 3.10. Aeronautical radio-navigation beacon 79 MHz

The range 70-80 MHz is mainly reserved for radio-navigation for air-traffic, see figure 28. Very often these signals produce cross-modulation in low-noise/high gain pre-amplifiers.

### 3.11. FM radio 87.5-108 MHz

The FM-band is fully occupied with local transmitters leading to high noise level on all channels in the band, see figure 29. In many radio-telescopes this band has to be notched with a band-stop filter (FM-trap). Callisto software allows to 'jump' over the whole band and to ignore these channels.

### 3.12. Aeronautical communication 117-137 MHz

The aeronautical band is sporadically occupied but 24 h/day, see figure 30. The modulation is still ampli-

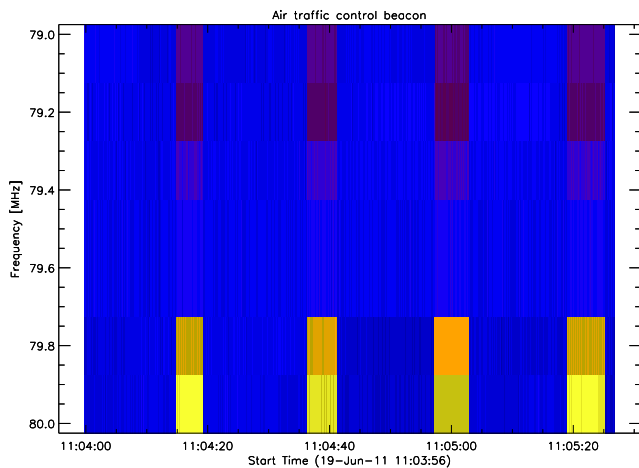


**Fig. 28.** Beacon of local airport used for radio-navigation. Period about 20 seconds with high transmission power.

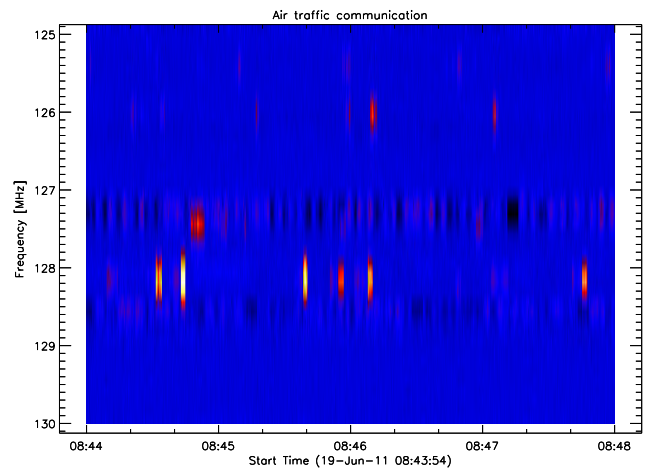


**Fig. 30.** Sporadic amplitude modulation from air traffic communication.

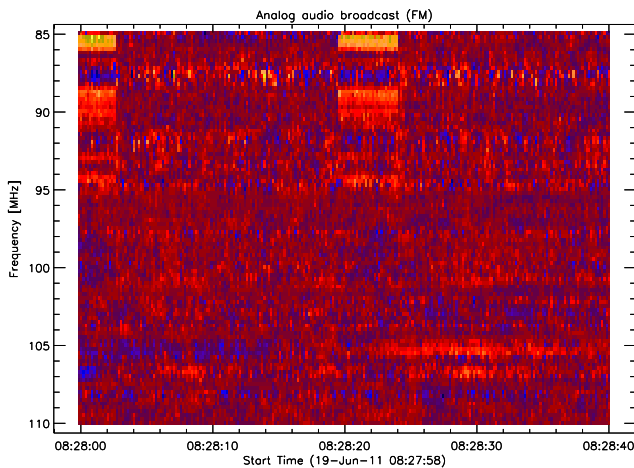


**Fig. 29.** FM (frequency modulation) band with full occupation of the band. All channels are nearly saturated.

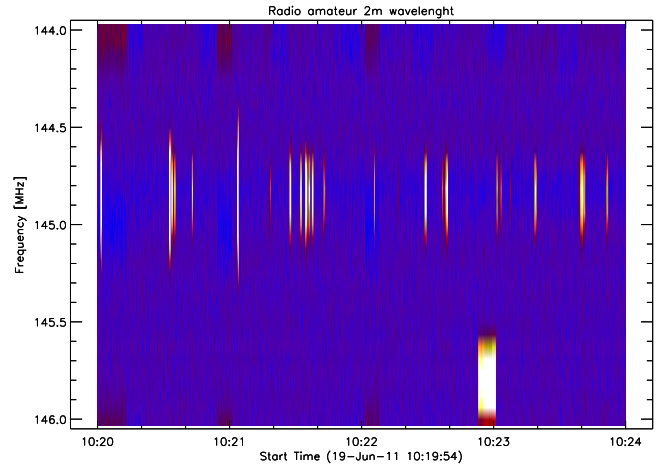


**Fig. 31.** Sporadic narrow frequency modulation (NFM) from amateur radio communication (HAM) in 2 m band.

tude modulation (AM) and may lead to saturation if the aeroplane is directly in beam of the antenna.

### 3.13. Radio amateur communication 144-146 MHz

HAM or radio amateurs have access to their own bands and use it for 24h/day, see figure 31. The power level is limited, therefore interference is limited to telescopes with nearby operators. The same range is also reserved for amateur satellites.

### 3.14. GENSO interference from 144-146 MHz transmission

The Global Educational Network for Satellite Operations (GENSO) is forming by a worldwide network of ground stations and spacecraft which can interact via a software standard. The GENSO aims to increase the return from educational space missions and changed the way that these missions are managed, dramatically increasing the level

of access to orbital educational spacecraft. Strong transmitters in 2 m band can produce harmonics 32nd and cross-modulation at higher frequencies.

### 3.15. Harmonics from military communication 146-148 MHz

Some badly designed military transmitter (non-linear power amplifier) can produce out of band interference (harmonics). Example observed near Cairo in Egypt, see figure 33.

### 3.16. Pager and tracking system 169.4-169.825 MHz

Permanent communication 24h/7d in narrow band frequency shift keying (NFM-FSK), see figure 34. These types of signal have strong influence to high gain pre-amplifiers and very often lead to saturation or cross-modulation. Some low frequency radio-telescopes need a notch-filter to suppress these signals.

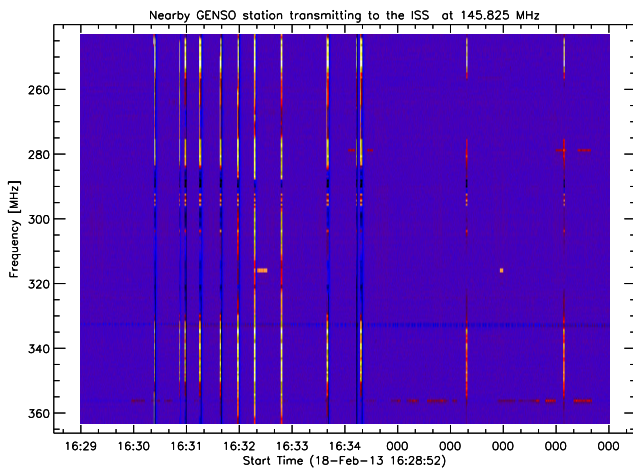


**Fig. 32.** Sporadic harmonics/cross-talk from strong amateur radio communication (GENSO) in 2 m band.

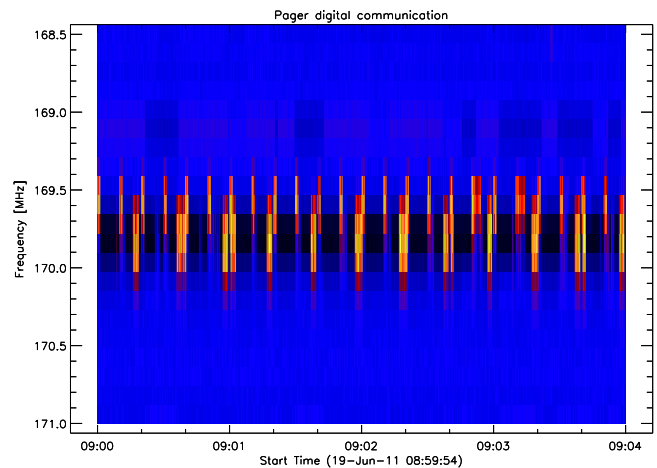


**Fig. 34.** Permanent communication in narrow band frequency shift keying (NFM-FSK).

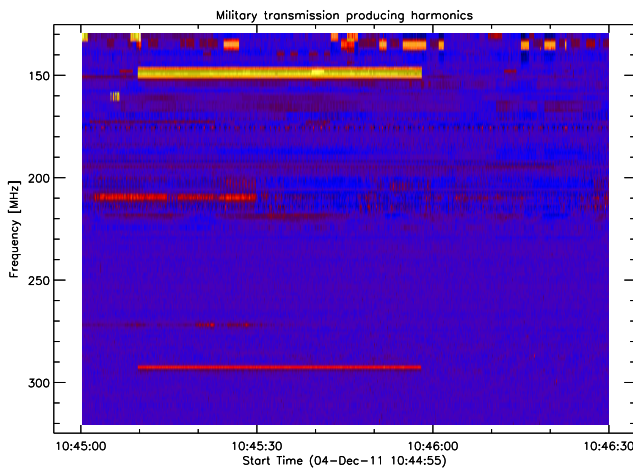


**Fig. 33.** Nearby military transmission around 147 MHz producing 1st harmonics at 294 MHz.

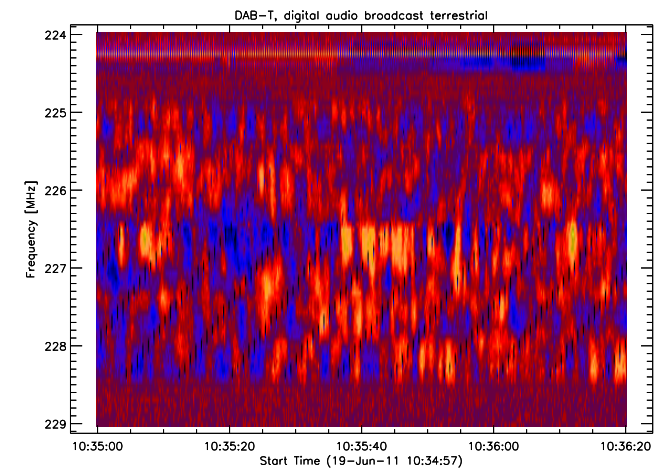


**Fig. 35.** Permanent (24h/7d) communication in digital audio broadcast terrestrial (DAB-T).

### 3.17. DAB-T 216-230 MHz

Digital terrestrial sound or television broadcast 24h/7d with high power and sharp edges in frequency range, see figure 35. Sometimes a phase locked structure can be recognized in the spectrum. Astronomical observations within DAB-channels are not possible.

### 3.18. Stationary (military) satellites 235-310 MHz

Many military satellites (MILSATCOM, UFO Follow On etc.) in geostationary position have down-link transponders in VHF-range, see figure 36. They are rather strong but there are always channels which are free and can therefore be used for observations. These transponders signals are very convenient for a quick check of the radio telescope. Under normal condition (antenna=log-per, low noise pre-amplifier without cooling) leads to a Y-factor of about 10 dB. This is the case for linear polarization, although the transponder are left circular polarized.

### 3.19. TETRA 380-395 MHz

(TERrestrial TRunked RAdio) is an international standard for digital mobile communications. TETRA systems are gradually being adopted in European countries by police forces and other emergency services. TETRA bears some resemblance to the digital mobile phone networks, but generally the cells are larger and the transmission powers higher. The introduction of any new transmission system is likely to cause some degree of interference to existing services, see figure 37. The problems caused to Radio-Astronomy and TV reception by TETRA, however, seem to be much more widespread than anyone anticipated. There are deep political issues involved with the implementation of TETRA. The frequencies allocated for police and fire service TETRA use are 380 - 385 MHz (mobile) and 390 - 395 MHz (fixed).

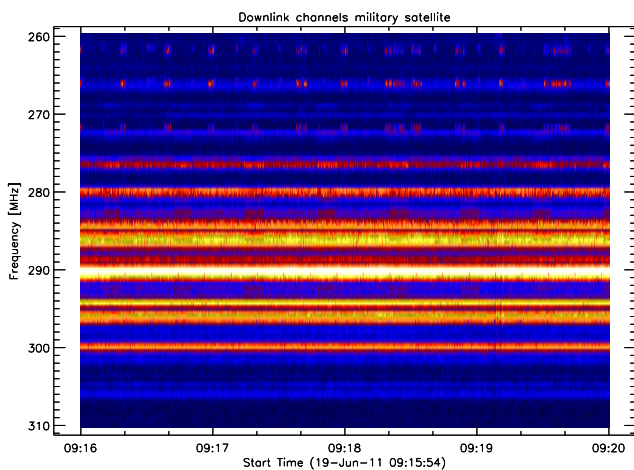


**Fig. 36.** Permanent (24h/7d) communication of military satellites.

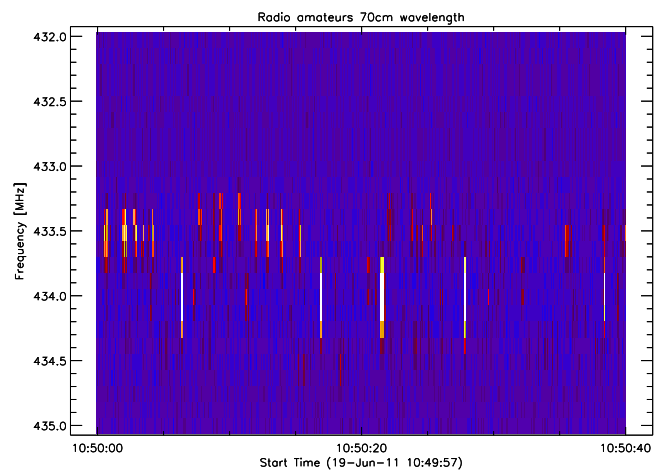


**Fig. 38.** Sporadic narrow frequency modulation (NFM) from amateur radio communication (HAM) in 70 cm band.

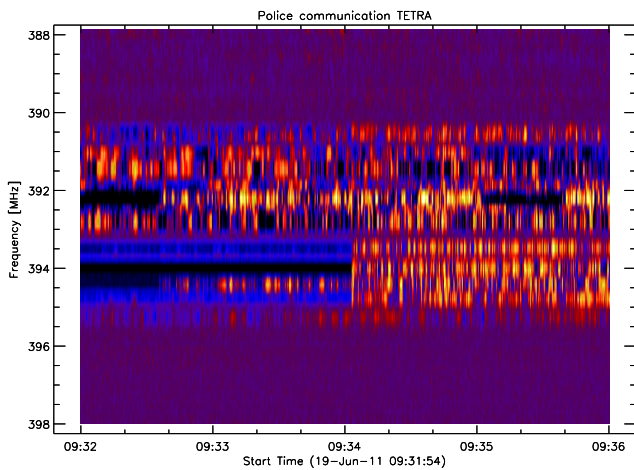


**Fig. 37.** TETRA, permanent communication 24h/7d in digital broad-band transmission.

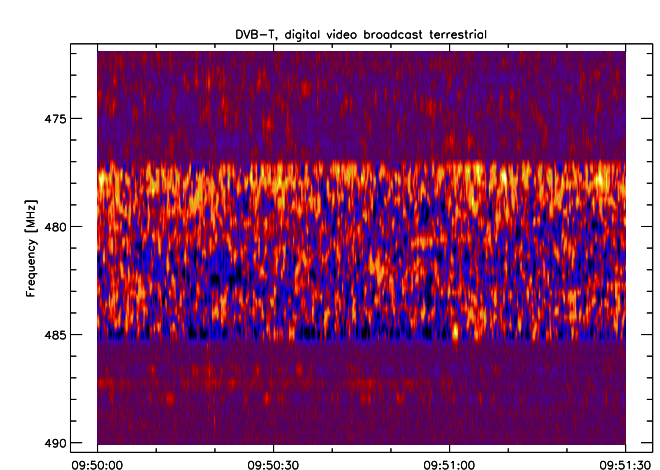


**Fig. 39.** DVB-T (digital video broadcast terrestrial, a permanent transmission in broad band technology).

### 3.20. Radio amateur communication 430-438 MHz

Shared 70 cm band mainly used by radio amateurs (HAM-operators) for communication, including amateur satellites. The power level is limited, therefore interference is limited to telescope sites with nearby operators. In the same band we can also see quasi periodic communication from remote (temperature) sensors, see figure 38.

### 3.21. DVB-T 470-608 MHz

DVB-T stands for terrestrial digital television broadcast and multi-media services. The spectrum shows very sharp edges at the border of the spectrum. In the band there is no chance for any radio-astronomical observations. The power level is very high without any structure in the spectrum, see figure 39. If zooming into the spectrum, it looks like a solar noise storm.

### 3.22. SRD 862-870 MHz

In telecommunication, a low-power communication device, also short-range device (SRD) is a restricted radiation device, exclusive of those employing conducted or guided radio frequency techniques, used for the transmission of signs, signals (including control signals), writing, images and sounds or intelligence of any nature by radiation of electromagnetic energy. Examples: Wireless microphone, radio-controlled garage door opener, and radio-controlled models. European licence-free LPD transceivers also include Short Range Device 860 MHz (SRD860), which have a maximum legal power output of 5 mW, see figure 40. SRD has a total of 126 channels in five bands. This kind of transmission can easily be mixed up with decimetric pulsations of solar bursts.

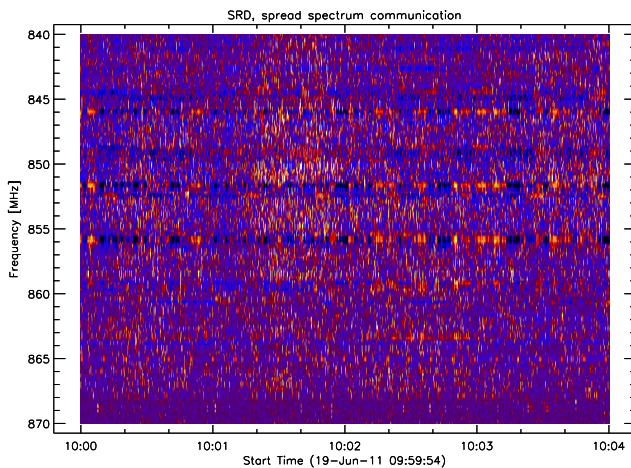


**Fig. 40.** SRD (short range device) band as broad band digital transmission 24h/7d looking like solar decimetric pulsations.

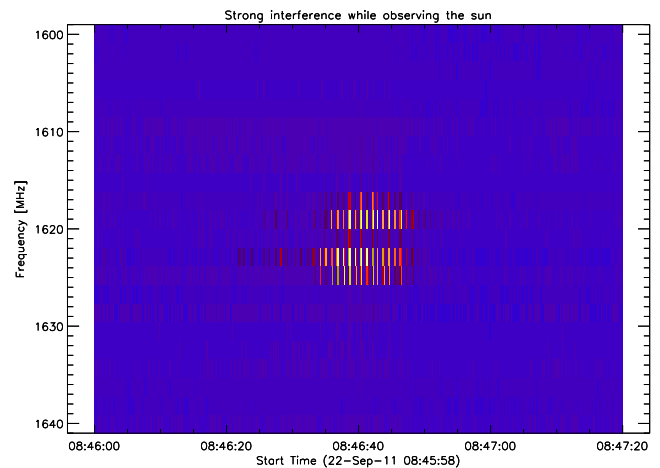


**Fig. 42.** Fast moving IRIDIUM satellite in the L-band near 1620 MHz observed at Bleien observatory Switzerland.

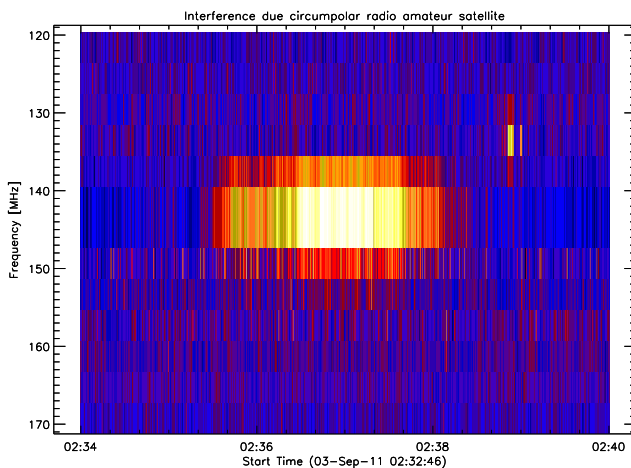


**Fig. 41.** Fast moving radio amateur (HAM) satellite in the 2 m VHF-band observed in Mauritius.

### 3.23. Non-stationary radio-amateur satellite

Typical spectrum of a fast moving radio amateur (HAM) satellite in the 2 m VHF-band near 145 MHz, see figure 41. The antenna beam of about  $90^\circ$  is crossed in about 2 minutes time. Observation from Mauritius radio telescope with a log-per antenna pointing to zenith.

### 3.24. Non-stationary IRIDIUM satellite

Typical spectrum of an IRIDIUM communication satellite in the L-band between 1611 MHz and 1630 MHz, see figure 42. The antenna beam of about  $2.5^\circ$  is crossed in about 30 seconds of time. Observation from Bleien radio telescope with a 5 m dish antenna while pointing to the Sun. This measurement was taken with the FFT-spectrometer Phoenix-3, therefore the low noise level outside of the satellite transponder signal. Radio astronomy has a primary allocation in the frequency band 1610.6-1613.8 MHz which covers an important spectral line of

hydroxyl (OH), one of the simplest and most common interstellar molecules (CRAF Newsletter 1999/2, 2004). The 1612 MHz line of OH is used by astronomers to investigate many astronomical processes, including the birth and death of stars, the evaporation of comets, and active nuclei in distant galaxies. The hydroxyl emissions come from regions which are hidden from optical telescopes by clouds of dust and gas. The OH 1612 MHz line is characteristic of a special class of astronomical sources, the OH-IR sources, which can only be studied through their hydroxyl and infrared emission.

### 3.25. Non-stationary weather satellite

Typical spectrum of a fast moving weather satellite in the L-band near 1697 MHz, see figure 43. The antenna beam of about  $2.5^\circ$  is crossed in about 20 seconds of time. Observation from Bleien radio telescope with a 5 m dish antenna pointing to the Sun. This measurement was taken with the FFT-spectrometer Phoenix-3, therefore the low noise level outside of the satellite transponder signal.

### 3.26. L-band radar pulses

L-band radar pulses reflected from a nearby building about  $10^\circ$  above the local horizon at Bleien observatory. Antenna 5 m dish pointing to the sky. Spectrometer is a FFT-instrument with 16'384 channels and 1 GHz bandwidth. Radar pulses are very regular in time with a period of about 10 seconds. Intensity is so strong that the spectrometer is getting saturated.

### 3.27. TACAN 'cigar burst'

A tactical air navigation system, commonly referred to by the acronym TACAN, is a navigation system used by military aircraft. It provides the user with bearing and distance (slant-range) to a ground or ship-borne station.

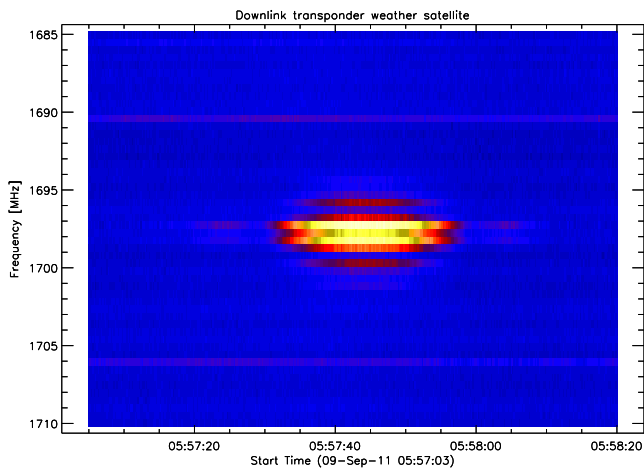


**Fig. 43.** Fast moving weather satellite in the L-band near 1697 MHz observed at Bleien observatory Switzerland .

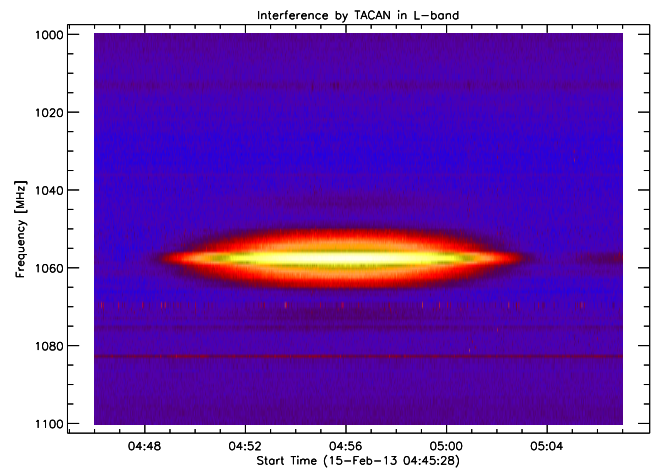


**Fig. 45.** TACAN signal from aircraft at 1057 MHz observed with Callisto on a 5 m dish at Bleien observatory Switzerland.

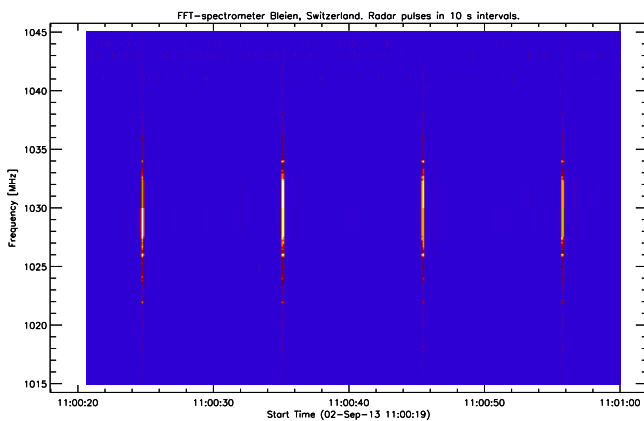


**Fig. 44.** Reflected radar pulse in the L-band at 1030 MHz observed at Bleien observatory Switzerland.

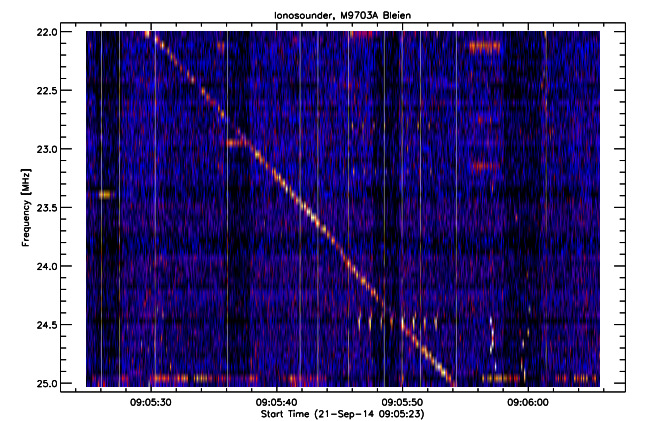


**Fig. 46.** Shortwave ionosonde observed with Long Wavelength Antenna (LWA) at Bleien observatory in Switzerland.

It is a more accurate version of the VOR/DME system that provides bearing and range information for civil aviation. Aircraft equipped with TACAN avionics can use this system for enroute navigation as well as non-precision approaches to landing fields. The space shuttle is one such vehicle that was designed to use TACAN navigation (although it has since been upgraded with GPS as a replacement). Rfi from TACAN needs almost 10 MHz of bandwidth, see figure 45. Luckily they are observed only 2 or 3 times per day with current beam-width of the antenna.

### 3.28. Ionosonde/Chirpsounder

An ionosonde, or chirpsounder, is a special radar for the examination of the ionosphere. An ionosonde consists of a high frequency (HF) transmitter, automatically tunable over a wide range. Typically the frequency coverage is 0.5 ... 23 MHz or 1 ... 40 MHz, though normally sweeps are confined to approximately 1.6 ... 12 MHz. A tracking HF receiver which can automatically track the frequency of the transmitter. An antenna with a suitable radiation pattern, which transmits well vertically upwards and is

efficient over the whole frequency range used. Digital control and data analysis circuits. The transmitter sweeps all or part of the HF frequency range, transmitting short pulses. These pulses are reflected at various layers of the ionosphere, at heights of 100 ... 400 km, and their echoes are received by the receiver and analyzed by the control system. see figure 46

### 3.29. Drone

A hexacopter drone was used to calibrate the beam pattern of the 5 m dish at Bleien observatory. Unexpectedly, the drone produced more broad band rfi than the attached calibration source underneath the drone, see figure 47. This is most probably due to high pulsed dc-current from flight control of the 6 motors.

### 3.30. Lawn cutter

An ordinary lawn cutter was used to cut grass near and around the antenna of CALLISTO at the Observatory of University of Glasgow, UK. Antenna is a LPDA, followed

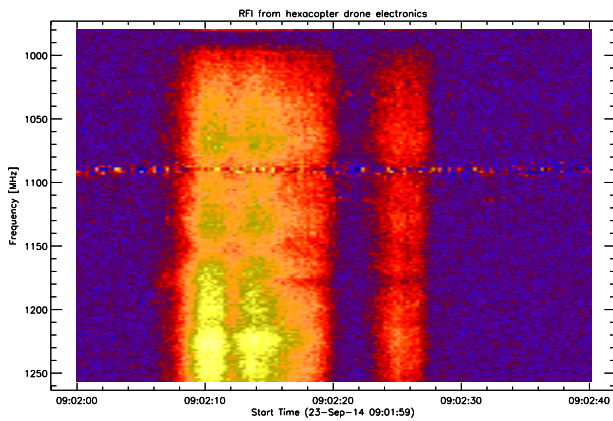


**Fig. 47.** Hexacopter drone flying above the 5 m dish at Bleien observatory Switzerland. The high current electronics produces broad band RFI.

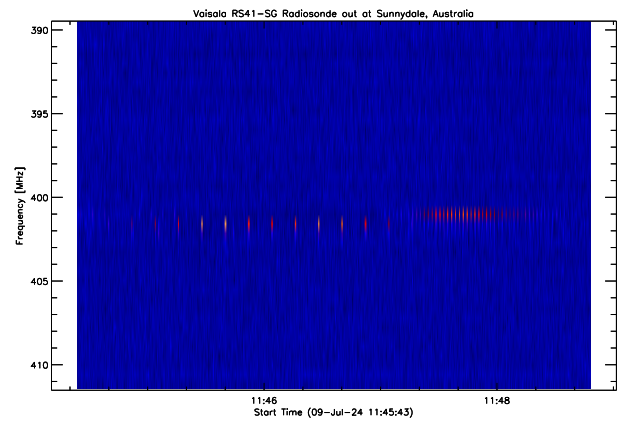


**Fig. 49.** RFI from weather balloon Vaisala RS41-SG Radiosonde out at Sunnysdale, Australia.

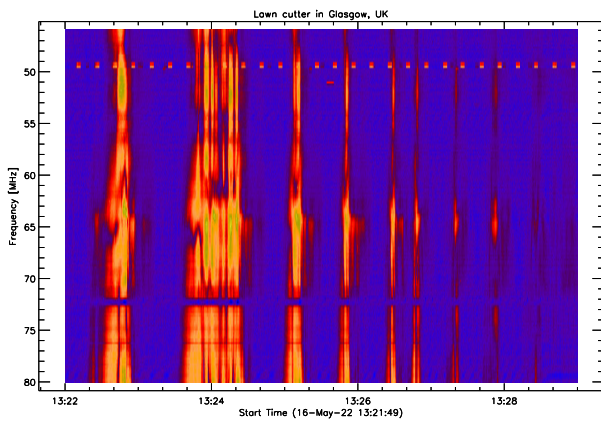


**Fig. 48.** Lawn cutter at observatory of University of Glasgow, UK. The strong current of drive electronics produces broad band RFI.

by a LNA from Mini circuits, see figure 48. This type of rfi is most probably due to high pulsed dc-current from cutting drive. Event looks like a group of type III bursts but, it's purely man-made.

### 3.31. Balloon

Encounter with a Vaisala RS41-SG Radiosonde out at Sunnysdale, Australia. The radiosonde passed at about 5.5 km altitude and just 500 m to the west of the ASSA-spectrometers but unfortunately, the radiosondes launched from Adelaide Airport transmit at 401.5 MHz which is above the current scanning frequencies 49. Therefore the scanning range was changed to observe this balloon with CALLISTO. After sunset they reconfigured their MWA antenna spectrometers (focuscodes 56 and 57) to scan between 225 MHz and 450 MHz, beginning at 1130 UT and finishing at 1400 UT. The upper frequency of 450 MHz is beyond the specified 370 MHz limit of the MWA antenna but reception of 401.5 MHz should be reasonably good and adequate for the purpose of this test. The purpose of this test is to determine if the signals they

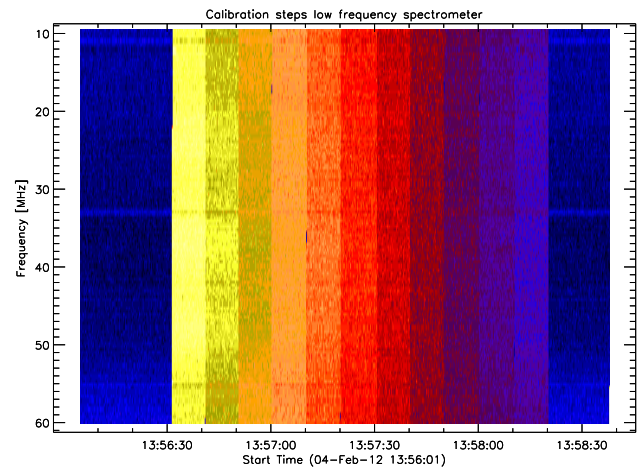


**Fig. 50.** Calibration steps generated by an adjustable attenuator from 0 dB in steps of 1 dB up to 10 dB) applied to low frequency Callisto. Intensity bars yellow=hot, red=warm and blue=cold.

often noticed around 400 MHz on the LPDA antenna spectrometer were the result of weather balloon flights.

## 4. Technical/instrumental problems

### 4.1. Spectrometer calibration

Example for a typical calibration process to check sensitivity and non-linearity of the complete spectrometer path including up-converter. In this case, see fig 50 we have an heterodyne up-converter from 10 MHz up to 80 MHz which move the spectrum into the VHF band 210 MHz to 280 MHz. The noise source is a semiconductor source with ENR=35 dB.

### 4.2. Data loss

Data loss can happen due to inappropriate resource of the control-PC, see figure 51. In most cases the virus-scanner (e.g. Sophos) took too much memory and too much processor resources. More general, the main reasons are:

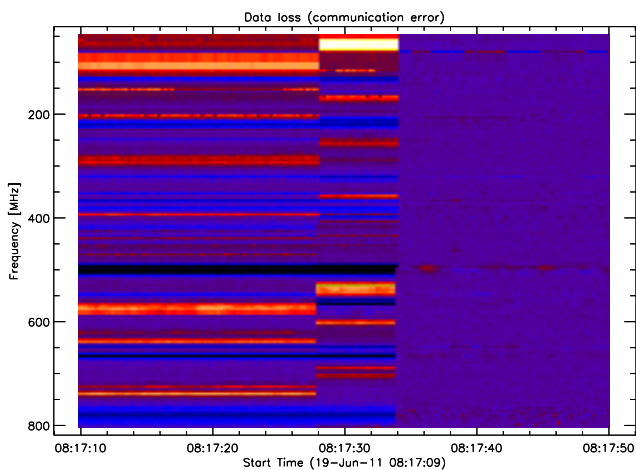


**Fig. 51.** Twice data loss near 08:17:30 UT due to inappropriate resources of an old PC.

1. bad quality of the RS-232 cable or a too long cable.
2. bad quality of RS-232/USB converter
3. bad selection of interrupt level
4. not enough working memory (RAM)
5. too many applications running on the PC
6. PC with insufficient resources

The effect is, that the spectrum jumps in frequency. In this case all channels are wrong.

#### 4.3. Interference due to self-excitation

The observatory at Birr (Ireland) castle was extremely suffering from self excited interference due to a worst case combination of total gain and isolation. The amplifier has a gain  $s_{21}$  of 21 dB and a reverse gain  $s_{12}$  of -24 dB. Together with the gain of the antenna of about 6 dB we get a self-exciting system which is also a function of output termination of the amplifier, see figure 52. The problem could be solved by switching in an attenuator of 3 dB between preamplifier and Callisto spectrometer. Finding the problem took several month. Once found, a solution was easy to implement.

#### 4.4. Unstable antenna positioning

Flux fluctuations at all frequencies, see figure 53 in the order of  $\pm 3\%$  in the S-band from 2000 MHz to 3000 MHz observed at Bleien observatory Switzerland with FFT-spectro-polarimeter Phoenix-3. The current beam in S-band is in the order of the antenna pointing-error leading to flux fluctuations. Either all the mechanics need to improved and also the resolution of the angle encoder on both axis. Or, a smaller dish-diameter leading to a larger beam would solve the problem.

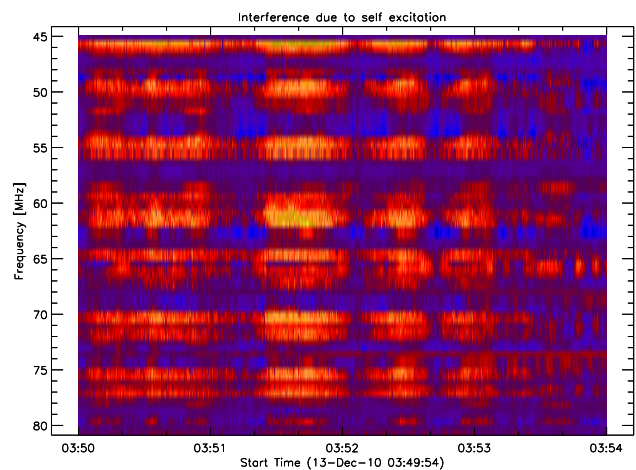


**Fig. 52.** Self excited system due to bad shielding and high gain amplifier.

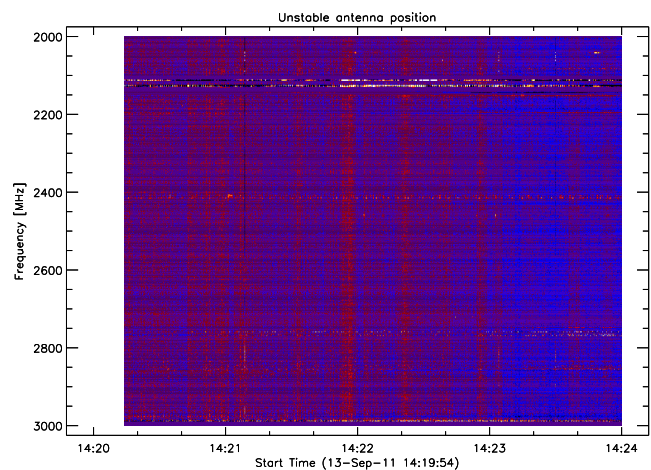


**Fig. 53.** Flux fluctuations (vertical stripes) in the S-band observed at Bleien observatory Switzerland with FFT-spectrometer Phoenix-3.

#### 4.5. Interference from overloaded power supply

Background fluctuations at all frequencies and all times, see figure 54 due to an inappropriate, cheap power supply with insufficient low pass filtering. It's worth to spend a high quality linear power supply instead of a low cost switched power supply. In the example below the power supply was specified for 500 mA, while Callisto only consumes 250 mA. So, a safety factor of two is not sufficient, a factor of 4 would be much better.

#### 4.6. Interference from badly filtered sewing machine

Here we have very strong interference produced by a badly filtered sewing machine. Motor brushes should have been filtered (low pass filter) to get rid of rfi, see figure 55 produced from sparks between brushes and collectors. Observations from Reeve observatory in Anchorage,

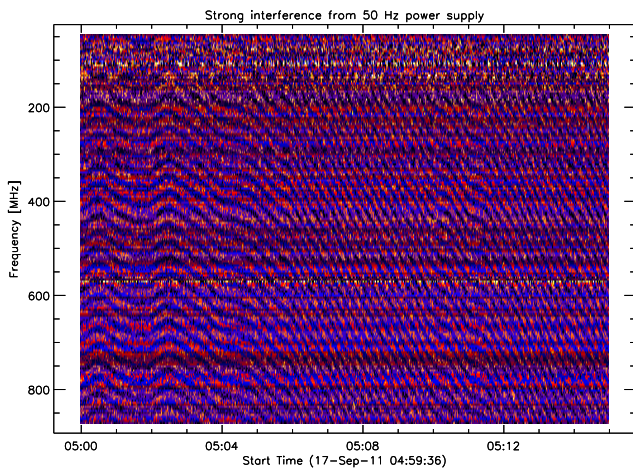


**Fig. 54.** Wobbling cords (50 Hz) due to a cheap, overloaded power supply.

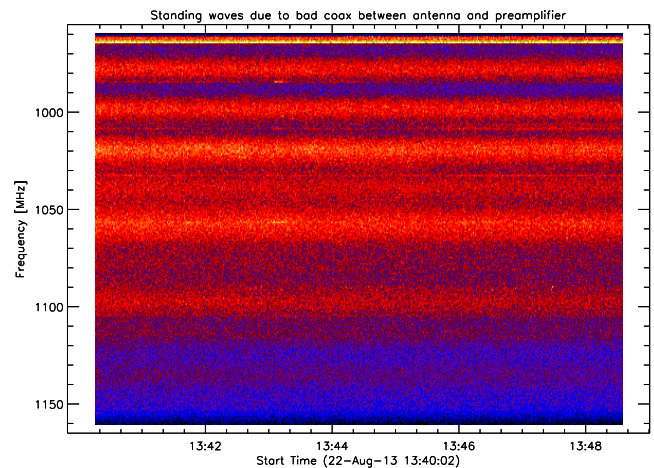


**Fig. 56.** Interference introduced by unmatched components in the high frequency path standing waves (SW).

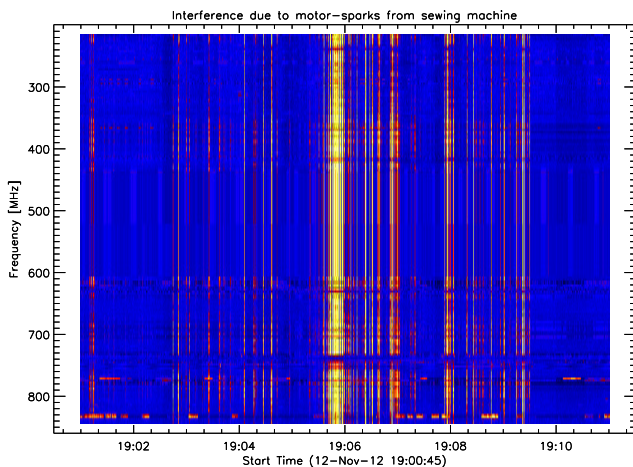


**Fig. 55.** Strong rfi produced by badly filtered sewing machine.

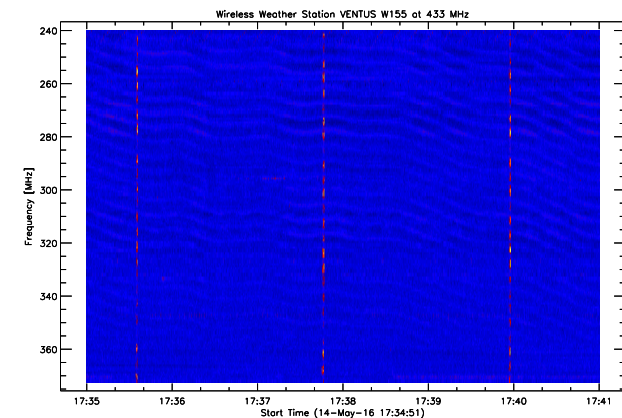


**Fig. 57.** Interference introduced by a badly designed nearby wireless weather station.

Alaska. Antenna CLP-5130 connected to a Callisto spectrometer.

#### 4.7. Standing waves due to bad impedance matching

A badly matched coax cable or badly designed antenna can produce interference, called standing waves (SW), see figure 56. All components should have the same impedance for electro-magnetic waves, e.g.  $50\Omega$ .

#### 4.8. Interference of a wireless weather station

A badly designed transmitter of a wireless weather station VENTUS W155, transmitting at 433 MHz produces strong interference below the carrier frequency. The weather data update rate is typically two minutes, producing these vertical stripes in the spectrum.

## 5. Unknown strange spectral sources

In some very rare cases we detected spectral structures which cannot be explained because they have never been observed before.

### 5.1. Mickey Mouse or ET

In July 2016 Callisto spectrometer in Mexico (station MEXART) observed twice a very strange dynamic spectra in VHF-range. The structure looks like Mickey Mouse. Either purely random rfi produced this events or clever students were able to construct a rf-source which can produce several frequencies at the same time such that such a structures results, see figure 58.

### 5.2. Weak Signal Propagation Reporter (WSPR)

WSPR is a weak signal slow speed short wave operation. When transmitting, operator usually set frequency up for 7.03860 MHz and 10.13870 MHz USB at a power level of 1 W to 5 W. In principle this low frequency signal should not

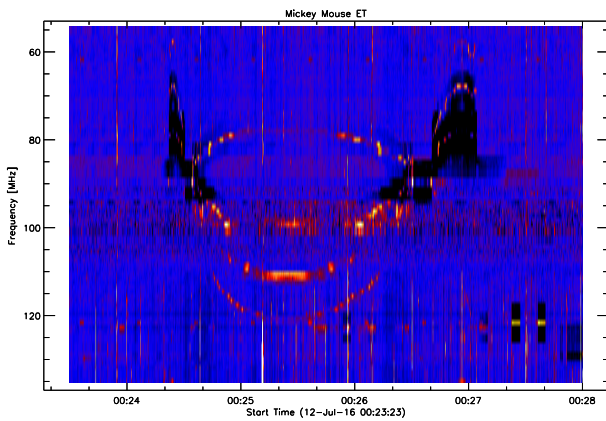


**Fig. 58.** Interference of a completely unknown source, denoted as Mickey Mouse.

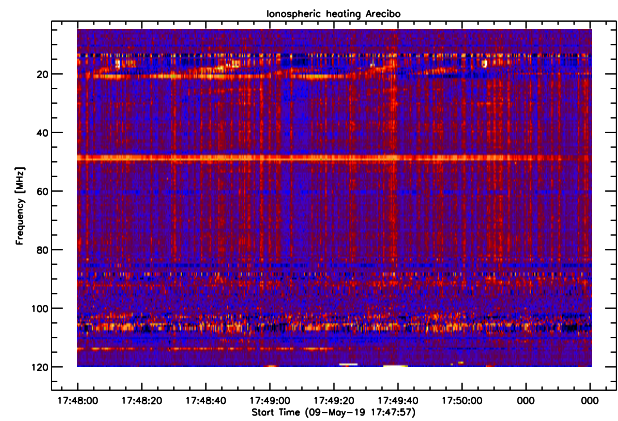


**Fig. 60.** Interference due to ionospheric heating at Arecibo Observatory.

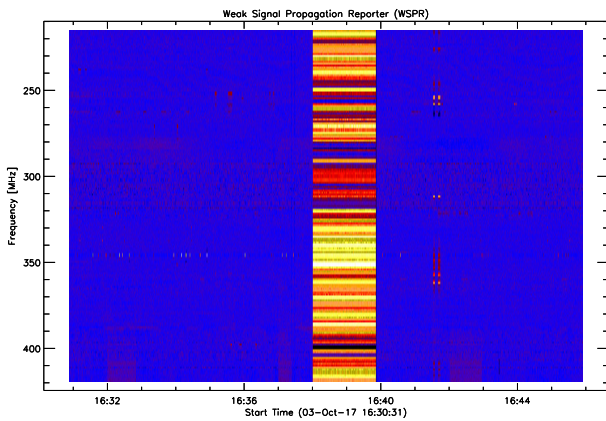


**Fig. 59.** Interference generated by a WSPR transmission.

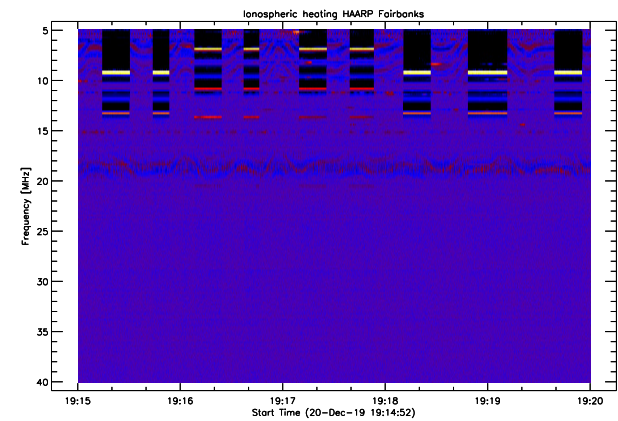


**Fig. 61.** Interference due to ionospheric heating at HAARP site in Gakona.

interfere at VHF/UHF unless the amplifier is saturated and produces harmonics, see figure 59.

### 5.3. Ionospheric heating Arecibo

Vertical stripes in this spectrum was generated to very powerful heating of the ionosphere at Arecibo Observatory in Puerto Rico, see figure 60. Transmitter frequency was 5.125 MHz with 500 watts of power inside the 305 m dish. Transmitter is outside the frequency band of Callisto and the receiving antenna was at least 200 m away and below the Arecibo dish antenna. Transmission is a HAARP-like experiment.

### 5.4. Ionospheric heating Gakona/Alaska

Vertical stripes in this spectrum were generated by powerful heating of the ionosphere at HAARP-site in Gakona, Alaska, see figure 61. Transmitter frequency was 6.8 MHz and 9.1 MHz with 6 kW of power. Transmission was just for testing with reduced power.

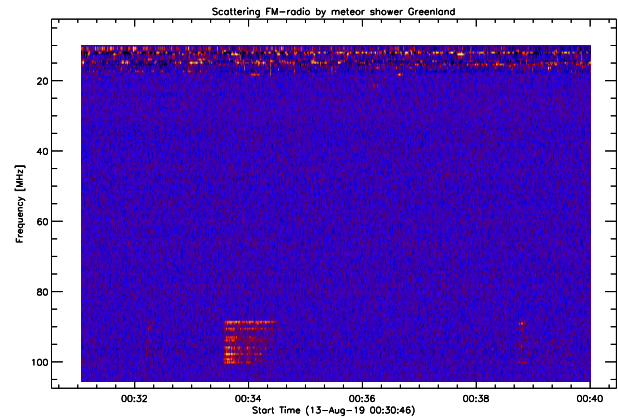


**Fig. 62.** Interference due to scattered FM-radio on meteor shower.

### 5.5. Meteor scatter

Scattering of remote FM-radio due to meteor shower in Greenland, see figure 62. A fast meteor shower entering the atmosphere generates a plasma which acts as a reflector. With this we can detect FM-radio which is out of line of sight.

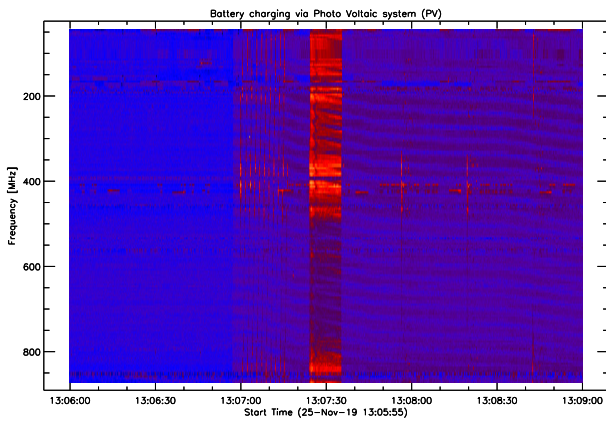


**Fig. 63.** Interference due to nearby photo voltaic power plant.

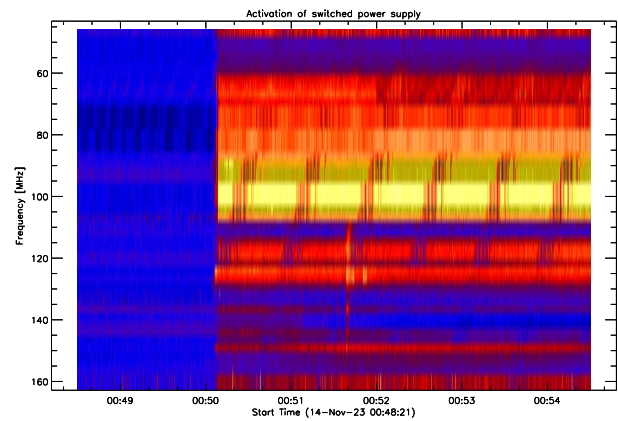


**Fig. 65.** Wide band interference due to power supply of the spectrometer 4-8 GHz at SSRT.

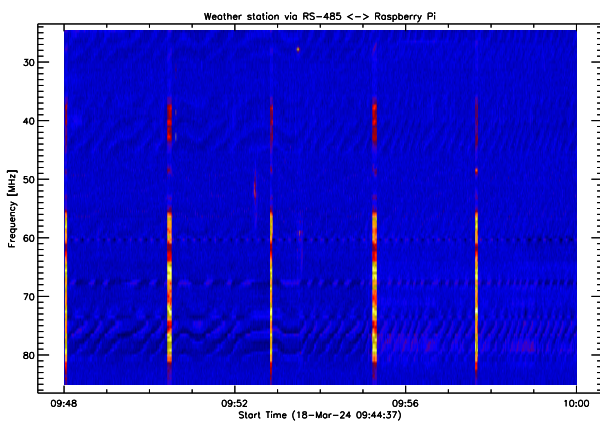


**Fig. 64.** Interference due to weather station connected to RaspBerry Pi.

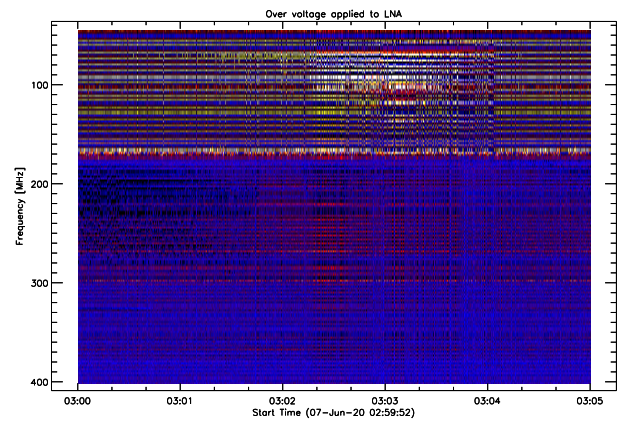


**Fig. 66.** Very strong interference due to too high voltage supply of the LNA.

### 5.6. Photo voltaic power supply

Wide band interference due to nearby photo voltaic power plant at Boumerdes observatory in Algeria, see figure 63. Testing and charging of battery show different wide band rfi. In this case the Callisto LPDA was moved away from interfering PV by about 60 m to mitigate rfi in the solar burst spectra.

### 5.7. Weather station on RaspBerry Pi

Wide band interference due to nearby weather station which is connected via a RS-485 interface to a RaspBerry Pi mini-computer, see figure 64. Data stream every 3 minutes generates this kind of wide band noise.

### 5.8. Power supply at SSRT

Strong, wide band interference due to power supply of the spectrometer 4-8 GHz at Siberian Solar Radio Telescope (SSRT), see figure 65. Every morning when the power supply was switched on, the level of rfi was more than 20 dB above background level at certain frequencies. And in the evening, when the power supply was switched off the spectrum went clean again.

### 5.9. Over voltage of LNA

Wide band and very bright rfi due to over voltage supply of the low noise amplifier (LNA), see figure 66. By accident the LNA and CALLISTO were supplied by a laboratory power supply with 32 volts instead of 12 volts. Except the front-LED CALLISTO survived but the LNA started to oscillate with high RF-power was measured with a spectrum analyzer at the input of CALLISTO with +30 dBm! Changing power supply solved the problem.

### 5.10. Interference by WiFi

Strong, wide band interference due to nearby WiFi internet-connection for FTP data upload to the central CALLISTO-server. Remote station without cable internet at Sunydale in Australia, see figure 67

## References

Mukul R. Kundu *Solar Radio Astronomy*, Interscience[Wiley], New York, 1965.

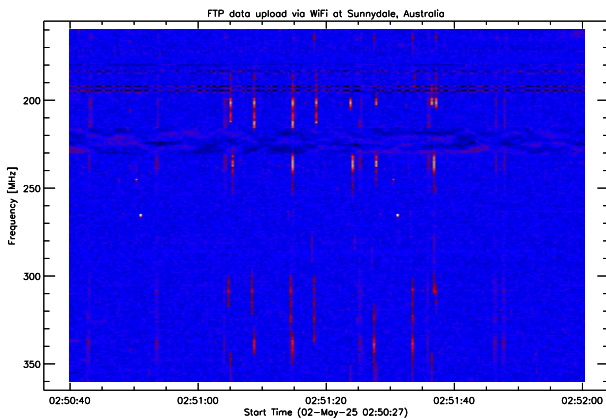


**Fig. 67.** Wide band interference due to a nearby WiFi internet connection.

Acronym	Explanation
AM	Amplitude Modulation
CME	Coronal Mass Ejection
DAB-T	Digital Audio Broadcast Terrestrial
DVB-T	Digital Video Broadcast Terrestrial
ESA	European Space Agency
ETH	Eidgenössisch Technische Hochschule
FFT	Fast Fourier Transform
FM	Frequency Modulation
FRB	Fast Radio Burst
FSK	Frequency Shift Keying
GENSO	Global Educational Network for Satellite Operations
GPS	Global Positioning System
HAARP	High Frequency Active Auroral Research Program
HF	High Frequency
ISWI	International Space Weather Initiative
LHCP	Left Hand Circular Polarization
LPD	Low Power Device
LPDA	Logarithmic Periodic Dipole Array
MRT	Mauritius Radio Telescope
NFM	Narrow band Frequency Modulation
NOAA	National Organization of Atmospheric Administration
OFCOM	Office Of Communication
RHCP	Right Hand Circular Polarization
rfi	Radio Frequency Interference
SRD	Short Range Device
SW	Standing Wave / Short Wave
TACAN	Tactical Air Navigation
TETRA	TErrestrial Trunked RAdio
TID	Traveling Ionospheric Disturbances
UHF	Ultra High Frequency
VHF	Very High Frequency
WiFi	"Wireless Fidelity" = W-Land

**Table 1.** Acronyms mentioned in text, images and plots.

Albrecht Krüger *Introduction to Solar Radio Astronomy and Radio Physics*, D. Reidel Publishing Company, Dordrecht, 1979.

Arnold O. Benz, Christian Monstein and Hansueli Meyer *CALLISTO, A New Concept for Solar Radio Spectrometers*, Kluwer Academic Publishers, The

Netherlands, 2004.  
*CRAF Newsletter 1999/2, May 1999, http :  
 //www.craf.eu/nwsl9902.htm#r.a.s.*  
 Maxwell A. and Swarup G. *A new spectral characteristic in solar radio emission*, Nature 181, 36 - 38 (04 January 1958), 1958.